JVI Journals.ASM.org

Host Gene Expression Is Regulated by Two Types of Noncoding RNAs Transcribed from the Epstein-Barr Virus BamHI A Rightward Transcript Region

Aron R. Marquitz,[a] Anuja Mathur,[a] Rachel Hood Edwards,[a] Nancy Raab-Traub[a,b]

Lineberger Comprehensive Cancer Center[a] and Department of Microbiology and Immunology,[b] University of North Carolina at Chapel Hill, Chapel Hill, North Carolina, USA

ABSTRACT

In Epstein-Barr virus-infected epithelial cancers, the alternatively spliced BamHI A rightward transcripts (BARTs) are the most abundant viral polyadenylated RNA. The BART introns form the template for the production of 44 microRNAs (miRNAs), and the spliced and polyadenylated exons form nuclear non-protein-coding RNAs. Analysis of host cell transcription by RNA-seq during latency in AGS cells identified a large number of reproducibly changed genes. Genes that were downregulated were enriched for BART miRNA targets. Bioinformatics analysis predicted activation of the myc pathway and downregulation of XBP1 as likely mediators of the host transcriptional changes. Effects on XBP1 activity were not detected in these cells; however, myc activation was confirmed through use of a myc-responsive luciferase reporter. To identify potential regulatory properties of the spliced, polyadenylated BART RNAs, a full-length cDNA clone of one of the BART isoforms was obtained and expressed in the Epstein-Barr virus (EBV)-negative AGS cells. The BART cDNA transcript remained primarily nuclear yet induced considerable and consistent changes in cellular transcription, as profiled by RNA-seq. These transcriptional changes significantly overlapped the transcriptional changes induced during latent EBV infection of these same cells, where the BARTs are exclusively nuclear and do not encode proteins. These data suggest that the nuclear BART RNAs are functional long noncoding RNAs (lncRNAs). The abundant expression of multiple forms of noncoding RNAs that contribute to growth regulation without expression of immunogenic proteins would be an important mechanism for viral oncogenesis in the presence of a functional immune system.

IMPORTANCE

Infection with Epstein-Barr virus (EBV) is nearly ubiquitous in the human population; however, it does contribute to the formation of multiple types of cancer. In immunocompromised patients, EBV causes multiple types of lymphomas by expressing viral oncogenes that promote growth and survival of infected B lymphocytes. EBV-positive gastric carcinoma does not require immune suppression, and the viral oncoproteins that are frequent targets for an immunological response are not expressed. This study demonstrates using transcriptional analysis that the expression of various classes of viral non-protein-coding RNAs likely contribute to the considerable changes in the host transcriptional profile in the AGS gastric cancer cell line. This is the first report to show that the highly expressed polyadenylated BamHI A rightward transcripts (BART) viral transcript in gastric carcinoma is in fact a functional viral long noncoding RNA. These studies provide new insight into how EBV can promote transformation in the absence of viral protein expression.

Latent infection with Epstein-Barr virus (EBV), a nearly ubiquitous human herpesvirus, is responsible for multiple malignancies in the two types of cells that it infects: B lymphocytes and epithelial cells (1). The mechanism by which EBV leads to transformation depends on both the properties of the host cell and the state of the host immune system. Infection of primary B cells with EBV *in vitro* is sufficient for immortalization, which results from the expression of a set of latent viral proteins that have oncogenic properties (1). This type of latent protein expression, termed latency III, is also observed in EBV-driven lymphomas that develop in immunocompromised individuals. In EBV-associated lymphomas or carcinomas that develop in individuals with a healthy immune system, a much more restricted pattern of viral protein expression is observed (2). However, these tumors are clonally infected with EBV, suggesting that EBV infection is an early event in the formation of the tumors (3). Consistent with these observations, EBV infection of an epithelial cell line *in vitro* is capable of promoting growth in soft agar independent of any latent protein expression (4).

EBV epithelial malignancies, nasopharyngeal and gastric carcinomas, exhibit a unique expression pattern that includes extensive transcription from the BamHI A region of the viral genome (5). The transcription from this region consists of a set of highly expressed and alternatively spliced transcripts that are called the BamHI A rightward transcripts (BARTs) (6). These transcripts

Received 8 June 2015 **Accepted** 21 August 2015

Accepted manuscript posted online 26 August 2015

Citation Marquitz AR, Mathur A, Edwards RH, Raab-Traub N. 2015. Host gene expression is regulated by two types of noncoding RNAs transcribed from the Epstein-Barr virus BamHI A rightward transcript region. J Virol 89:11256–11268. doi:10.1128/JVI.01492-15.

Editor: R. M. Longnecker

Address correspondence to Nancy Raab-Traub, nrt@med.unc.edu.

Supplemental material for this article may be found at http://dx.doi.org/10.1128/JVI.01492-15.

Copyright © 2015, American Society for Microbiology. All Rights Reserved.

contain multiple open reading frames (ORFs) dependent upon splicing pattern (BARF0, A73, and RPMS1); however, proteins have not been detected from the endogenous translation of these ORFs (7, 8). A first clue to the actual function of these transcripts came from the discovery that the introns of these transcripts contained 22 microRNA (miRNA) precursors which can produce 44 mature miRNAs, many of which are expressed at high levels in tumors, the same tumors that also express the BARTs (9–11). Analysis of the residual RNA fragments that remain after excision of the miRNA hairpins suggests that these miRNAs are removed from the primary transcript prior to splicing (12). Despite this, the spliced and polyadenylated mature transcripts persist at high levels in epithelial cells and have been shown to remain in the nucleus (8, 12). A recent RNA-seq analysis of a panel of EBV-infected gastric tumors suggested that >99% of all virally derived polyadenylated transcripts were BARTs (13, 14).

Infection of the EBV-negative gastric carcinoma cell line AGS is a useful model for studying EBV epithelial latency since these cells consistently adopt a highly restricted pattern of expression that is quite similar to latency I in EBV-positive gastric carcinoma. Importantly, EBV infection of AGS cells consistently induces anchorage-independent growth and increased motility (4, 15, 16). Gene expression microarray analysis of a single AGS-EBV cell line compared to parental cells suggested that there are widespread changes in host transcription due to latent EBV infection and that the downregulated genes were highly enriched for BART miRNA targets (4). In the present study, multiple clonal AGS-EBV cell lines were profiled by RNA-seq, generating data that are more accurate than data obtained by microarray analysis, that account for the clonal evolution inherent in any one particular cell line, and that include an evaluation of not only host but also viral transcription. Pathway analysis identified multiple cellular regulatory pathways that are consistent with anchorage-independent growth and transformation. The transcriptional changes predicted activation of the myc oncogene which would likely be a contributing factor to the altered growth properties. In addition, RNA-seq analysis of AGS cells expressing the first full-length cDNA clone of one of the splice isoforms of the BARTs revealed that the expression pattern obtained after BART expression overlapped significantly with the expression pattern following EBV infection of the same cells in which the BARTs are expressed at high levels endogenously. These data provide the first evidence that the BARTs function as long noncoding RNAs (lncRNAs) independently of miRNA formation. Human lncRNAs are quite abundant in the human genome, with recent evidence from RNA-seq and other sources suggesting that there are likely nearly as many lncRNA genes as protein coding genes in the human genome (17). Many of the functions of these lncRNAs have yet to be determined, although those for which a functional mechanism has been determined often rely on transcriptional regulation through direct recruitment either of transcription factors or chromatin remodeling enzymes (18). The transcriptional regulatory functions of the BARTs, independent of miRNA production, and their abundance in EBV derived epithelial malignancies suggest that these noncoding RNAs likely contribute to EBV effects on epithelial growth and transformation.

MATERIALS AND METHODS

Cell lines and culture. The gastric carcinoma cell line AGS was grown in F-12 media (Life Technologies, Inc.) with 10% fetal bovine serum and antibiotic/antimycotic (Life Technologies, Inc.). The generation of AGS cells clonally infected with EBV Akata BX1 was previously described (15). AGS-EBV cells were also maintained with 500 μg of G418 (Life Technologies, Inc.)/ml to select for retention of the EBV episome. Stable cell lines expressing pcDNA3-BART were generated by transfection with Lipofectamine 2000 (Life Technologies, Inc.) and selected in media containing zeocin (Life Technologies, Inc.) at 200 μg/ml. Cell lines containing pCEP4 episomal vectors were maintained in 200 μg of hygromycin (Roche)/ml to select for retention of the vector. Normal oral keratinocyte (NOK) and NOK-Akata cells (a gift from Shannon Kenney, University of Wisconsin) have been previously described (19) and were maintained in keratinocyte-SFM (Life Technologies, Inc.) supplemented with epidermal growth factor, bovine pituitary extract, and antibiotic/antimycotic.

Plasmids and cloning. The myc reporter plasmid pBV-Luc wild-type (wt) MBS1-4 was a gift from Bert Vogelstein (Addgene, plasmid 16564) and contains four tandem myc binding sites from the human CDK4 promoter upstream of Firefly luciferase (20). pBV-Luc mut MBS1-4, a gift from Bert Vogelstein (Addgene, plasmid 16565), which has all four myc binding sites mutated (20), was used as a negative control. pRL-SV40 (Promega) is a *Renilla* luciferase-expressing plasmid that was used as a transfection control. The full 3′ untranslated regions (3′UTRs) of potential miRNA targets were amplified by PCR from genomic AGS DNA using Phusion Flash High Fidelity PCR mix (Thermo) and cloned into the XhoI/NotI sites of psicheck2 (Promega). The oligonucleotides used to amplify each 3′UTR are listed in Table S3 in the supplemental material. In order to create a full-length BART cDNA clone, a cDNA PCR product from exon 1 to exon 7 (positions 138353 to 160086 on the wt EBV genome [NC_007605.1]) previously generated from cDNA from a nasopharyngeal carcinoma xenograft (12), was extended to the poly(A) site of the BARTs using overlap PCR with a PCR fragment of exon 7b. The oligonucleotides 5′BARTlong and 3-5exon7b were used to amply the first fragment from the cDNA clone, and the oligonucleotides 3′BARTlong and 5-3exon7b were used to amply the exon7b fragment. After overlap PCR using these two PCR products and oligonucleotides 5′BARTlong and 3′BARTlong, the resulting PCR product was cloned into the BamHI and XhoI sites in the multiple cloning site of pcDNA3.1-zeo (Life Technologies, Inc.). The resulting plasmid was sequenced and confirmed to contain a full-length BART cDNA that contains exons 1, 1A, 2, 3A, 3B, 4, 5A, 5B, 6, 7A, and 7B (see Fig. 5). In order to move the BART cDNA into the pCEP4 vector (Life Technologies, Inc.), the entire cDNA was excised from pcDNA3 by cutting with KpnI/XhoI and inserted into the pCEP4 multiple cloning site cut with the same enzymes. All restriction enzymes were purchased from NEB and used according to the manufacturer's instructions.

RNA sequencing. RNA was prepared from cell lines grown for 2 days to 80% confluence using TRIzol reagent (Life Technologies, Inc.). Poly(A)-selected, bar-coded, non-strand-specific cDNA libraries were prepared for sequencing using a TruSeq RNA Sample Prep kit v2 (Illumina) by the UNC Lineberger Genomics Core. Libraries were pooled and sequenced in pools of six libraries using a HiSeq2000 instrument (Illumina) by the UNC High-Throughput Sequencing Facility. AGS parental, AGS-EBV, and AGS with pcDNA3 vectors were sequenced using paired-end 100-bp sequencing, and the pCEP4 cell lines were sequenced using paired-end 50-bp sequencing. Raw data for all of the sequencing are publicly available at the NCBI short read archive under study SRP060253.

Bioinformatics. RNA sequencing reads were aligned to the human genome (hg19) and the EBV Akata genome (GenBank accession number KC207813.1) using the splicing aware read aligner TopHat on the Galaxy suite. Aligned reads were mapped to specific human Refseq genes using the Partek Genomics Suite, which was also used to calculate differentially expressed genes, generate hierarchical clusters, and perform principle component analysis. In order to visualize the reads representing the BART cDNA clone, reads that did not map to the human genome using TopHat were mapped the Akata genome using Bowtie. Aligned reads were visualized using the Integrative Genomics Viewer (21). Enriched molecular functions and potential upstream regulators for the AGS-EBV data set

were obtained by running a core analysis on the differentially expressed genes using Ingenuity Pathway Analysis (IPA) software (Qiagen).

Luciferase assays. Cell lines were grown to confluence in six-well dishes and transfected with the appropriate vectors using Lipofectamine 3000 (Life Technologies, Inc.). At 48 h posttransfection, the cells were lysed and assayed using the dual-luciferase report assay system (Promega) on a Glomax 96 instrument (Promega). For the myc activity assays, 2.7 μg of the pBV-MBS1-4 reporter and 300 ng of the control pRL-SV40 vector (Promega) were transfected into each well. For the 3′UTR assays, 500 ng of the indicated psicheck2 vector was transfected into each well.

UPR assay. AGS or AGS-EBV cells were plated into six-well plates at a density of 10^6 cells per well 24 h before assay and cultured at 37°C. The cells were treated with 40 μM, 200 μM, 1 mM, or 5 mM dithiothreitol (DTT) for 4 h at 37°C and then harvested for RNA preparation using TRIzol reagent (Life Technologies, Inc.). An XBP1 splice isoform was assayed from each RNA sample by using reverse transcription-PCR (RT-PCR) with a Qiagen Quantifast One-Step RT-PCR system and the primers 5′XBP1 and 3′XBP1 (see Table S1 in the supplemental material). This PCR generates a 249-bp product from the unspliced RNA and a 223-bp product from the spliced RNA. PCR fragments were resolved on an agarose gel to distinguish between these two sizes.

Western blotting. Protein lysates were prepared from cells, and Western blot analysis was performed as previously described (22). Primary antibodies used were mouse α-c-myc (Santa Cruz, sc-40) and rabbit α-GAPDH (Santa Cruz, sc-25778).

Quantitative RT-PCR. RNA was prepared from cell lines using TRIzol reagent (Life Technologies, Inc.). Quantitative RT-PCR was performed using the Quantifast SYBR green RT-PCR kit (Qiagen) on a QuantStudio 6 Flex real-time PCR system (Applied Biosystems) with primers designed for each gene tested. In order to detect the BART lncRNA, two sets of primers were designed: one that spans the exon 4-exon 5 junction (primers exon4R and exon5aL) and one that spans the exon 6-exon 7 junction (primers exon6R and exon7aL) (see Table S1 in the supplemental material). In both cases, the specific PCR product was only detected in EBV-positive cells or cells containing the BART cDNA. RNA from specific cellular fractions was isolated by using a differential lysis technique, followed by TRIzol prep, as previously described (12). The percentage of transcript in the nucleus was calculated from the relative abundance obtained from cycle thresholds using quantitative RT-PCR from an equal volume of cytoplasmic and nuclear RNA. The primers to amplify specific human transcripts are listed in Table S1 in the supplemental material and are identified by the names of the respective genes. These primer pairs were designed with the help of the NCBI primer blast, and each span an exon-exon junction of the mature transcript and are predicted to have no off targets in the human transcriptome. In all cases the reported differential expression is based on the differences in cycle threshold of control versus experimental, normalized to the differences in cycle threshold of a GAPDH reaction used as a control.

RESULTS

EBV effects on cellular expression. In order to better understand the effects of latent EBV infection in epithelial cells, RNA-seq was used to obtain a complete transcriptional profile of both uninfected and infected AGS cells. mRNA libraries were generated using the Illumina TruSeq RNA prep kit to obtain libraries from RNA isolated from three preparations of uninfected AGS cells, one EBV-infected cell line obtained that has been previously profiled by microarray (4), and two additional EBV-infected AGS cell lines that have been recently generated (15). Sequence reads generated by paired-end, 100-bp sequencing on the Illumina HiSeq 2000 instrument were aligned to both the human (hg19) and the Akata EBV (KC207813) genomes by using the splicing aware read aligner Tophat. Human alignments were matched to annotated RefSeq transcripts using the Partek genomics suite software. It was possible to align the vast majority of reads in this sequencing to the human genome and most of those reads mapped as pairs to RefSeq transcripts (Table 1). Consistent with the fact that the infection in these cells is mostly latent, only a small percentage of the mappable reads correspond to EBV, ranging from 0.19 to 0.48%. A recent report examining lytic induction of an EBV-positive Burkitt's lymphoma cell line by RNA-seq suggested that lytic cells can produce ca. 7% of the total sequence reads derived from the virus (23), which would correspond to a background lytic activation of around ~5% if similar transcription levels occurred in lytic AGS cells.

TABLE 1 Summary of RNA-seq reads

Cell line	No. of reads		
	Total	Mapped to human	Aligned human pairs[a]
AGS#1	42,799,160	39,755,541	17,974,295
AGS#2	61,878,112	57,253,646	25,869,971
AGS#3	52,469,526	48,625,673	21,987,733
AGS-EBV#1	49,800,978	45,650,825	20,641,133
AGS-EBV#2	62,470,636	59,981,567	27,159,052
AGS-EBV#3	64,846,600	57,285,114	25,909,124
pcDNA3#1	87,435,366	82,832,788	37,784,366
pcDNA3#2	75,886,016	71,854,311	32,795,626
pcDNA3#3	70,694,780	66,720,313	30,458,784
pcDNA3-BART#1	64,859,972	61,276,130	28,004,326
pcDNA3-BART#2	66,423,548	62,190,749	28,266,128
pcDNA3-BART#3	72,997,746	68,396,572	31,001,562
pCEP4#1	66,755,870	60,509,879	25,812,976
pCEP4#2	70,824,278	67,749,126	29,677,147
pCEP4#3	67,247,644	64,586,394	28,196,855
pCEP4-BART#1	49,707,074	46,745,211	20,092,075
pCEP4-BART#2	77,541,962	72,745,999	31,912,940
pCEP4-BART#3	51,382,276	48,593,505	21,287,109

[a] That is, the number of read pairs that correctly align together on a known RefSeq transcript.

It is clear from the analysis of the RNA-seq results that latent infection with EBV reproducibly alters the transcription pattern of AGS cells. Principle component analysis revealed that the original AGS-EBV cell line obtained from the Hutt-Fletcher lab has a pattern of transcription that is distinct from the two AGS-EBV cell lines generated more recently in our lab (Fig. 1A). This likely reflects the continuing clonal evolution that occurs in these cell lines during extended passage. However, hierarchical clustering revealed a large number of consistent changes were common to all three lines, indicating that latent EBV infection modulates host cell transcription, and the induced changes can be distinguished from those that reflect clonal variation between cell lines (Fig. 1B). After filtering out the lowest expressed transcripts, there were 1,514 genes upregulated and 715 genes downregulated with a P value of <0.05 (Fig. 1B; see also Table S2 in the supplemental material). Of these changes, 53 upregulated and 101 downregulated genes were changed >2-fold after EBV infection. The transcriptional changes associated with EBV infection were enriched in genes with functions related to cell growth and proliferation, cell death and survival, and gene expression (Fig. 1C). The changes in expression observed predicted that the infected cells would have an increase in proliferation and cell viability and a decrease in apoptosis and cell death, which is consistent with the increased

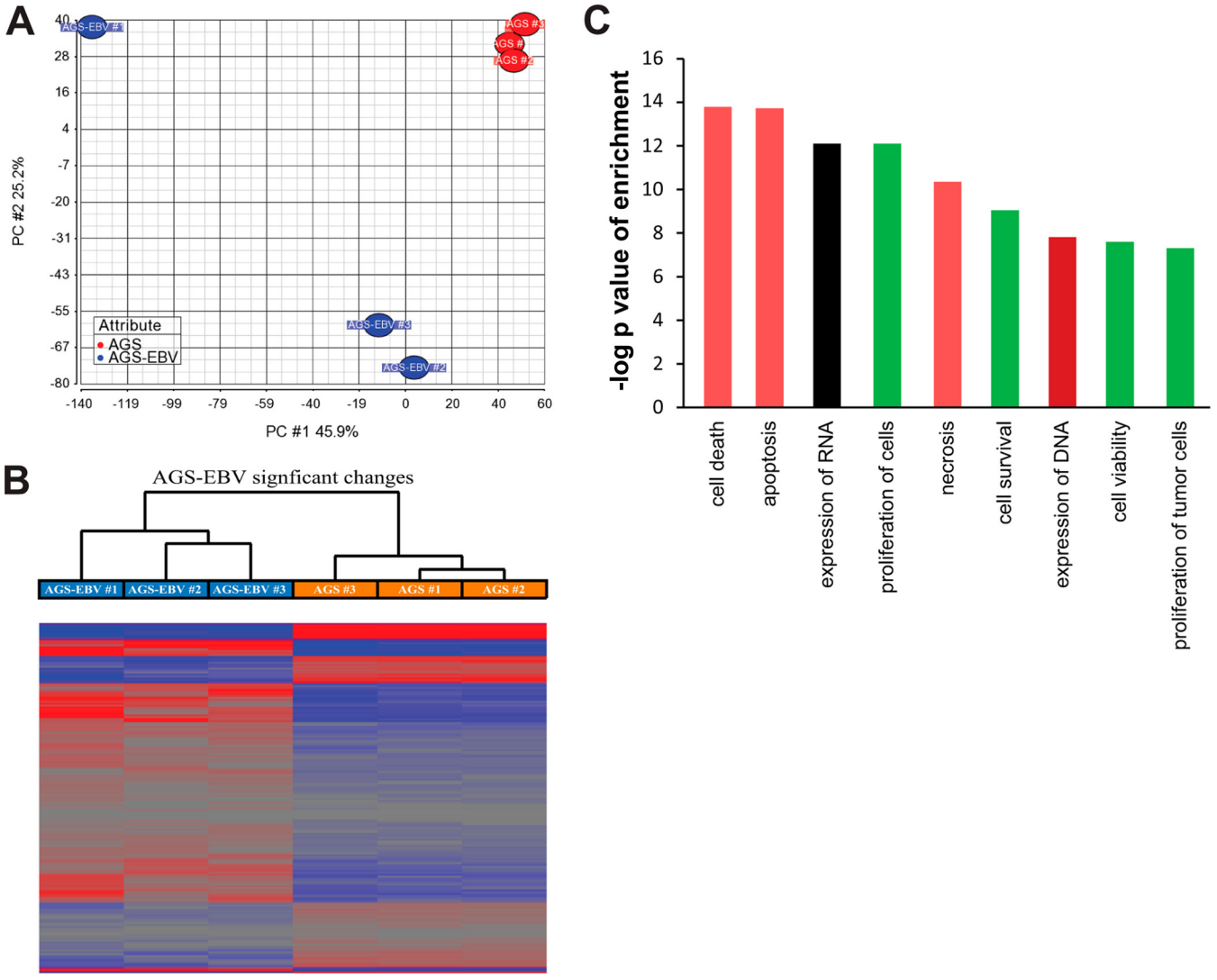

FIG 1 RNA-seq analysis of AGS cells following EBV infection. (A) Principle component analysis of variation between all expressed transcripts from AGS cells. The red circles represent three replicate libraries from the AGS parental cells, and the blue circles represent three libraries for independent AGS-EBV cell lines. The blue circle in the top left of the graph represents the original AGS-EBV cell line obtained from the Hutt-Fletcher lab, and the two blue circles at the bottom of the graph represent two independently generated clonal EBV-infected cell lines. (B) Hierarchical clustering of genes significantly changed by EBV infection. The 2,229 genes significantly changed ($P < 0.05$) after EBV infection were clustered independently. Red indicates expression higher than the mean of the six libraries, and blue indicates expression lower than the mean. (C) IPA software was used to classify genes regulated by EBV infection into categories based on the known molecular function of the genes. Graphed are categories that were highly enriched in the data sets, with the size of each bar corresponding to the −log of the *P* value of enrichment. Green bars indicate that the function is predicted to be activated, and red bars indicate that the function is predicted to be inhibited based on the pattern of expression of these genes. Black bars indicate that the function can be predicted to be neither activated nor inhibited based on the data.

anchorage-independent growth previously observed in these cell lines (4, 15).

In order to determine whether the transcription changes were caused by a discrete subset of activators and/or repressors, the Ingenuity Pathway Analysis (IPA) software package was used to query possible upstream regulators that could account for these transcription changes. This analysis suggested that myc, the glucocorticoid receptor (NR3C1), and the insulin receptor were increased in activation and the stress response transcription factor XBP1, Rb, the inflammatory kinase MAP4K4, and the transcription factor p8 (NUPR1) were decreased in activation (Fig. 2A). These predictions had highly significant *P* values, reflecting the degree of overlap with the genes in the data set and significant Z scores indicative of activation or repression. To confirm activation of the myc pathway, a luciferase reporter construct containing a 200-bp region of the CDK4 promoter with four myc binding sites was used to assess myc activity in the parental AGS line, as well as five independent clonal EBV-infected lines. As a control, the activity of the reporter construct with mutations of all four myc binding sites was also assessed. In four of the five lines tested (including lines 1 and 2, which were analyzed in the RNA-seq experiment), the myc activity was higher than in the parental lines (Fig. 2B). Mutation of the myc sites greatly reduced the reporter activity. The activation of myc occurred despite a minor decrease in the transcription of the MYC gene (see Table S2 in the supplemental material) and without a statistically signif-

A

Upstream Regulator	Activation Z-score	p-value of overlap
XBP1	-4.306	3.59E-10
INSR	3.267	3.12E-09
MAP4K4	-4.161	1.88E-07
MYC	4.032	8.46E-07
NR3C1	2.447	1.63E-05
NUPR1	-4.129	4.09E-05
IGF2	-2.401	2.93E-04
RB1	-2.798	7.68E-04

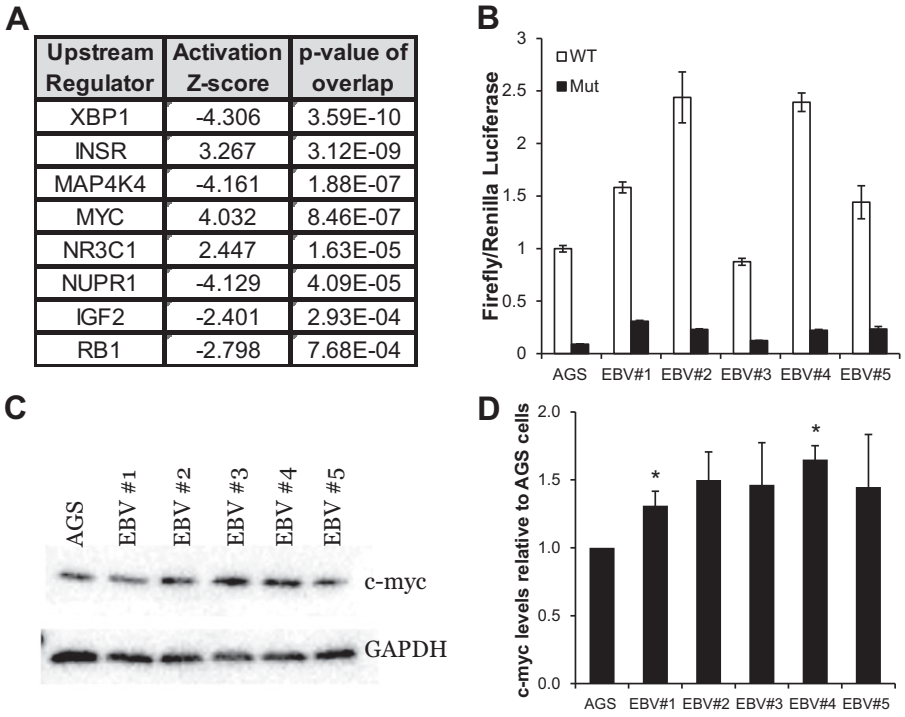

FIG 2 Latent infection of AGS cells with EBV induces myc transcriptional activity. (A) IPA software was used to predict upstream regulators of the significantly changed genes. The *P* value of overlap is a measure of how likely the overlap between genes in the data set, and genes targeted by the upstream regulator occurred at random. The activation Z score is an indication of whether the upstream regulator is activated or repressed based on the changes observed in the data set. The higher the absolute value of the Z score, the more likely the upstream regulator is affected, with positive Z scores indicating activation and negative Z scores indicating inhibition. The list shown is the most significant upstream regulators based on *P* value that have a Z score of >2, which is a cutoff for statistical significance. (B) AGS cells and five clonal AGS-EBV lines were transfected with a reporter with the four myc binding sites from the CDK4 promoter driving Firefly luciferase (wt) or a control reporter in which all four sites have been mutated (mut). A plasmid expressing *Renilla* luciferase was used as a transfection control. After 48 h, the cells were assessed for each luciferase activity, and the ratio of firefly/*Renilla* luciferase for the wt reporter in the parental AGS cells was set to 1. The assay was performed six times for the wt reporter and three times for the mutant reporter, and the graph represents the mean value, with error bars indicating the standard errors of the mean (SEM). (C) Western blot showing the levels of c-myc protein in each of the cell lines in panel B with GAPDH levels assessed as a loading control. (D) The average result of four independent c-myc Westerns normalized to GAPDH is plotted as the expression relative to the AGS control cells. Although there is a trend toward an increase in c-myc levels, none of these are statistically significant based on a one-sample *t* test. The asterisk represents a *t* test result of $P = 0.10$.

icant increase in c-myc protein levels, as assessed by Western blotting (Fig. 2C and D).

The IPA method also predicted that XBP1 is significantly inhibited despite being expressed at equivalent levels according to the RNA-seq data. XBP1 is a key regulator of the unfolded protein response (UPR) and is regulated by a cytoplasmic splicing event upon endoplasmic reticulum (ER) stress that results in a frameshift and the production of a more active transcription factor (24). To determine whether EBV infection affected the production of the spliced isoform of XBP1, the RNA-seq reads were examined across the locus (Fig. 3A). There was no decrease in reads across the XBP1 alternative splice, suggesting that in both AGS and AGS-EBV cells XBP1 exists in the unspliced and less active isoform. However, the RNA-seq analysis indicated that a large number of the genes activated during the ER stress response are inhibited following EBV infection. To assess the effects of EBV infection on the ability of XBP1 to respond to ER stress, AGS or AGS-EBV cells were treated with increasing amounts of DTT to induce the UPR, and XBP1 splicing was monitored by RT-PCR. In this assay, EBV did not affect the ability of XBP1 to be activated in response to ER stress (Fig. 3B). Taken together, these data suggest that although many of transcriptional targets of the UPR are downregulated in response to EBV infection, the mechanism of this downregulation is not the result of direct effects on XBP1 activation.

Potential effects of EBV miRNAs. AGS cells infected with EBV express high levels of the BART miRNAs (15), and previous profiling of one AGS line by microarray suggested that a substantial subset of the downregulated genes after latent infection were direct targets of the BART miRNAs (4). To confirm that the BART miRNAs contribute to the changes in gene expression profiled in the multiple infected cell lines in this report, the genes changed in expression were overlapped with the most extensive lists of BART miRNA targets published to date, where the BART miRNA targets were identified by PAR-CLIP in a peripheral effusion lymphoma cell line dually infected with EBV and KSHV, as well as the NPC cell line C666 (25, 26). A higher percentage of the downregulated genes and a lower number of the upregulated genes overlapped with the PAR-CLIP data sets compared to the null hypothesis, which would be the percentage of all genes expressed in AGS cells (based on the RNA-seq data) that overlap the PAR-CLIP data set (Fig. 4A and B). The decrease in expression is in accordance with expected effects of miRNAs. To determine whether some of the downregulated genes were direct targets of miRNAs, the 3′UTRs of several genes were cloned into a luciferase reporter vector.

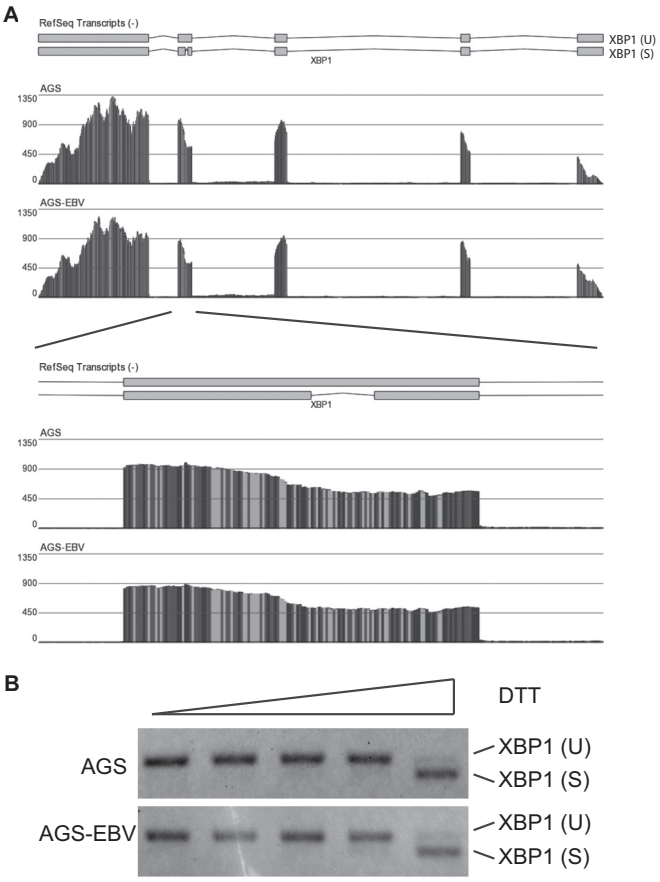

FIG 3 Regulation of XBP1 during EBV infection of AGS cells. (A) Graphical representation of the numbers of reads aligned across the XBP1 locus from AGS and AGS-EBV cells. At the top is an illustration of the structure of the XBP1 transcripts, in which the first exon is on the right. The XBP1(S) isoform results from a cytoplasmic removal of 26 nucleotides from the fourth exon, as indicated. The number of reads spanning each nucleotide is represented by the height of the bar in the histogram, and the shading of the bar represents the nucleotide identity. The lower histogram is zoomed in on just exon 4 showing reads spanning the internal splice. (B) AGS or AGS-EBV cells were treated with 40 μM, 200 μM, 1 mM, or 5 mM DTT for 4 h. Cells were then harvested, and the XBP1 splice isoform status was assessed by RT-PCR. The predicted sizes for XBP1(U) and XBP1(S) are indicated.

Given that the PAR-CLIP data set is derived from a very distinct cellular context and in order to potentially identify novel miRNA targets, a miRNA target prediction program (PITA) was also used to query the 3′UTRs from each downregulated gene against the top 15 BART miRNAs in terms of expression for predicted miRNA sites. From the resulting list of potential targets, the UTRs for nine genes (MXI1, GSTM, RASA1, CTNNA1, GPX2, DUSP6, PTPN6, JMY, and IER3) were cloned. CTNNA1, JMY, and IER3 were also identified as BART miRNA targets in the BC1 PAR-CLIP data set. These genes all have potential tumor suppressive functions, and thus downregulation might contribute to the increased transformation phenotype of these cells (Table 2). Of these nine selected genes, the 3′UTRs of eight of the genes, with the exception of RASA1, had significantly decreased activity in EBV-infected cells, although the results of IER3 fell just short of statistical significance (Fig. 4C). These data indicate that the BART miRNAs are likely responsible for some of the gene expression changes in the EBV-infected AGS cells. Interestingly, MXI1 is a negative regulator of myc, which may partially explain the activation of myc following EBV infection.

The spliced EBV BART RNA modulates cellular expression. Previous work has shown that the most abundant polyadenylated viral RNAs in EBV-positive gastric carcinoma samples are the spliced BART transcripts (13), which are also expressed at high levels in the AGS-EBV cells. Considerable evidence exists to suggest that the BARTs do not encode proteins (27), and previous studies have suggested that these transcripts are not exported to the cytoplasm (8, 12). However, these spliced transcripts from which the primary miRNA sequences contained within the introns are removed are quite abundant and stably remain in the nucleus. These properties suggest that the BARTs possibly function as noncoding RNAs in the nucleus, analogous to human lncRNAs. In order to determine whether the BART RNAs have a role independent of generation of miRNAs, a full-length cDNA clone was generated by overlap PCR from the longest BART cDNA successfully cloned from the C15 nasopharyngeal carcinoma xenograft (Fig. 5A and B) (12). This cDNA was repaired to include the 3′ sequences of exon 7 and the polyadenylation site using Akata DNA. This full-length 2-kb cDNA corresponding to one possible isoform of the BARTs was cloned into the mammalian expression plasmid pcDNA3 and the EBNA1 based episomal vector pCEP4 (Fig. 5A and B). Cell lines were generated by selecting for three independent stable integrations of the pcDNA3 vectors or three independent lines maintaining the episomal pCEP4-BART in AGS cells. Quantitative RT-PCR for the splices between exons 4-5 and exons 6-7a was used to determine the relative expression of the BART cDNA. The pcDNA3 lines expressed the BART cDNA to levels comparable to EBV-infected cells (Fig. 5C), while the pCEP4 lines expressed higher levels than the EBV-infected cells (Fig. 5D). Endogenous BART RNAs remain in the nucleus; therefore, the localization of the expressed cDNA clones was determined by nuclear fractionation of cells, followed by RNA preparation and quantitative RT-PCR. Importantly, a majority of the expressed RNA remained in the nucleus at levels comparable to the nuclear U5 RNA (Fig. 5E).

In order to determine the relative abundance of this particular BART isoform cloned from the cDNA in the AGS-EBV cells, the RNA-seq data aligned to the viral genome were analyzed for spliced reads. Because these data were generated from sequencing that cannot distinguish between strands, it is not possible to separate reads that derived from the BART region from reads that represent the lytic transcripts on the opposite strand from the BARTs. However, by tallying the number of reads that span the various splice junctions possible among the BARTs, it is possible to determine the abundance of various splice isoforms of the transcripts. In AGS cells there is a large variety of splicing events that occur at the 5′ end of the transcripts, but starting with exon 3, direct splicing of exon 3-4-5-6-7 appears to be by far the most abundant splice isoform (Fig. 6A). The alternative splicing events within exons 3, 5, and 7 that have been previously described (6) were also detected, although at a much lower abundance (Fig. 6A). These data are in good agreement with the previously published splicing analyses performed using EBV gastric carcinoma tumors and EBV-infected lymphocytes, suggesting that the splicing pattern of the BARTs is relatively constant during EBV latency (13, 28). These data suggest that the cDNA clone that was generated from the C15 tumor is also expressed in AGS-EBV cells, although

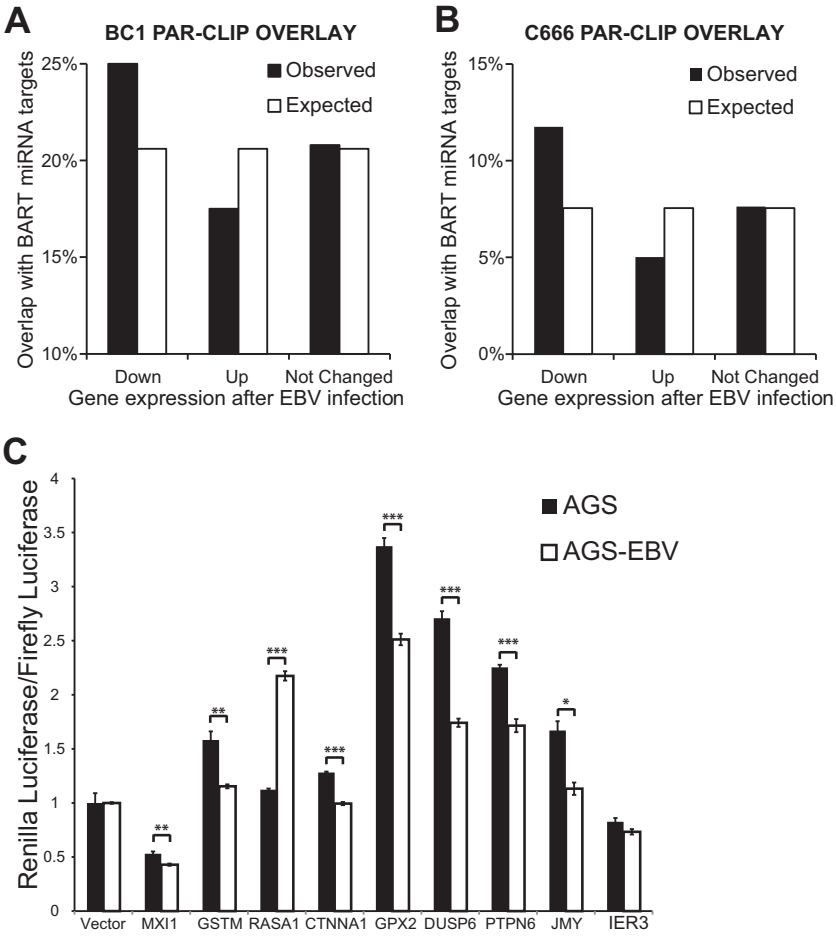

FIG 4 BART miRNAs contribute to the downregulation of cellular gene expression. (A) Bar graph showing the percentages of genes that overlap between the genes increased (Up), decreased (Down), or not changed after EBV infection and an experimentally determined set of BART miRNAs targets from BC1 cells. The overlapped observed is graphed in black, and the overlap expected if the BART miRNAs did not contribute to gene changes in graphed in white. This null hypothesis expectation is the fraction of genes expressed in AGS cells ($n = 11,476$) that also appear in the BART target data set ($n = 2,364$), which is 20.6%. (B) The same analysis performed from a BART miRNA target set from C666 cells. In this instance, there were 866 targets expressed in AGS cells, and thus the null hypothesis is 7.6%. (C) A 3′UTR luciferase reporter assay was performed. The entire 3′UTR for each of the indicated genes was cloned onto the coding sequence of *Renilla* luciferase in the psicheck2 vector, which also contains the firefly luciferase gene expressed as a separate transcript. Each resulting vector was transfected into AGS and AGS-EBV cells, and the activity of *Renilla*/firefly luciferase was measured at 48 h posttransfection. Plotted is the mean of three independent transfections, normalized to the ratio obtained from an empty vector in each cell line. The error bar represents the SEM. The asterisks refer to the results of a Student *t* test between the AGS and AGS-EBV samples (*, $P < 0.05$; **, $P < 0.01$; ***, $P < 0.001$). The IER3 assay had a *P* value of 0.055.

it is not the most abundant isoform. In order to predict what effect alternative splicing might have on the structure and thus the function of the BART RNAs, the RNAfold webserver was used to generate predicted structures for both the BART cDNA cloned for this study and the larger splice isoform that is most abundant based on RNA-seq and lacks the additional splicing within exons 3, 5, and 7 (Fig. 6B). The predicted structures suggest that the downstream splicing events in exons 3, 5, and 7 do not have major effects on the structure of the 5′ region of the RNA, suggesting that common functions for multiple splice isoforms may be possible. However, the additional sequences in the unspliced exons does dramatically change the base pairing in the 3′ region of the molecule, suggesting that each splice isoform might have unique functions dependent on the distinct secondary structure.

As a first attempt to understand whether the BART RNAs have a function in addition to being the template for miRNA production, the six independently derived cell lines containing the BART cDNA clone were subjected to RNA-seq, along with six empty vector control cell lines created in parallel. The use of six independently derived cell lines and six controls allows for considerable statistical power and enables the identification of changes due to the actual expression of the BART cDNA and not resulting from clonal variation. The sequencing was performed and analyzed identically to the EBV-infected cells, with the exception that the sequencing was 50-bp pair-end reads. The depth of coverage and percentage of reads aligning to the human reference genome were very similar to the previous sequencing (Table 1). In order to confirm expression of the full-length BART cDNA, the reads were also aligned to the Akata genome. The BART reads span the length of the clone as expected (see Fig. S1 in the supplemental material).

Analysis of the differential expression of genes between these libraries indicated that the major factor influencing expression was the type of expression vector used, and the expression of the BART cDNA was identified as the second greatest variable. How-

TABLE 2 Predicted BART miRNA targets downregulated in AGS-EBV cells

Gene	RNA-seq fold change	Predicted site(s)[a]		Fold 3′UTR reporter activity in AGS-EBV compared to AGS	Role as a tumor suppressor
		PITA-predicted miRNA target sites	PAR-CLIP-predicted miRNA target sites[b]		
MXI1	–1.19	BART 22-3p (7), BART19-3p (10)		0.81	Negative regulator of myc
GSTM	–1.21	BART10-3p (2)		0.73	Detoxification of carcinogens
RASA1	–1.07	BART10-3p (2)		1.94	Negative regulator of ras
CTNNA1	–1.22	BART12-3p (34)	BART5-5p (4)	0.78	Inherited mutation leads to gastric cancer
GPX2	–3.12	BART17-5p (8)		0.74	Prevents inflammation dependent tumors in gastric epithelium
DUSP6	–1.20	BART11-3p (9)		0.64	Negative regulator of ERK, activated by p53
PTPN6	–1.11	BART6-3p (6)		0.76	Negative regulator of tyrosine kinase signaling
JMY	–1.31	BART9-5p (5), BART19-3p (7), BART17-5p (8), BART11-3p (9), BART2-5p (17)	BART10-3p (2), BART5-5p (4), BART17-5p (8), BART18-3p (10), BART19-3p (13)	0.68	Coactivator of p53, helps integrate actin dynamics and adherens junctions to p53 function
IER3	–1.45	BART17-3p (14)	BART2-3p (42)	0.89	Stress-inducible gene that can downregulated NFκB, ERK, and Akt

[a] Numbers in parentheses represent the rank in terms of BART miRNA abundance in AGS-EBV cells according to previously published miRNA sequencing data (15).
[b] PAR-CLIP predicted BART targets, as determined previously (23).

ever, one pair of pCEP4 control and BART libraries was significantly different from all of the others (Fig. 7A). For subsequent analysis, these outliers were excluded, and the five remaining BART expressing cell lines were compared to the corresponding controls. Principle component analysis indicated that PC1 representing 46.2% of the variation between these 10 libraries was accounted for by the difference between the integrating and episomal vectors; however, PC2 representing 23.3% of the variation was directly due to BART cDNA expression (Fig. 7B). The large differences between the integrating versus episomal vectors is

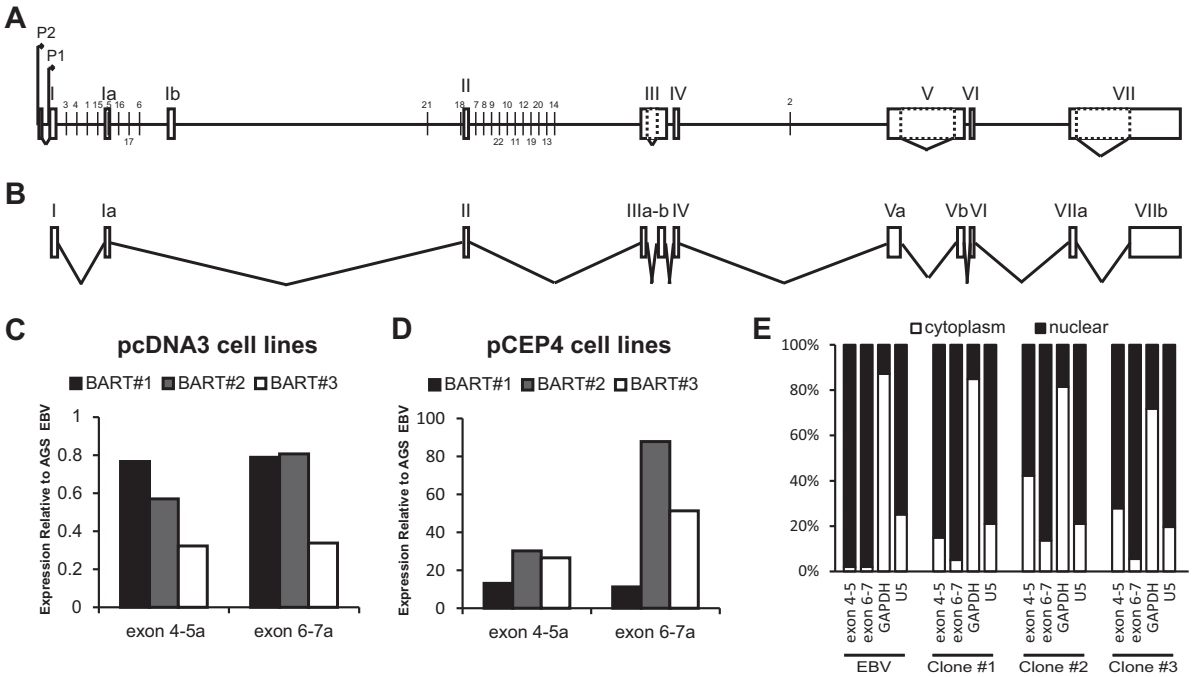

FIG 5 Expression of a Full Length BART cDNA. (A) Diagram of the BART locus. (B) Exon structure of the BART cDNA cloned into pcDNA3 and pCEP4 vector. (C) Expression of the BART cDNA clone in three independently derived, pcDNA3-based, stable AGS cell lines. Expression is measured by quantitative RT-PCR using primers that span the exon 4-5 or exon 6-7 junctions and is expressed relative the same PCR performed from AGS-EBV cells. (D) Expression of the BART cDNA from three independently selected cultures of AGS cells containing the episomal pCEP4-BART vectors. PCR was performed as described for panel C. (E) Nuclear fractionation of pcDNA3 stable lines to determine the localization of the expressed BART. Cells were fractionated into nuclei and cytoplasm, and RNA was prepared from both samples and subjected to quantitative RT-PCR using the same primers as in panels C and D, as well as primers recognizing GAPDH mRNA and the nuclear RNA U5 as controls. The results are expressed as the percentage of the PCR product derived from each of the fraction. As a control, AGS-EBV cells were also fractionated and show the expected localization of the BARTs and U5 in the nucleus and GAPDH mRNA in the cytoplasm.

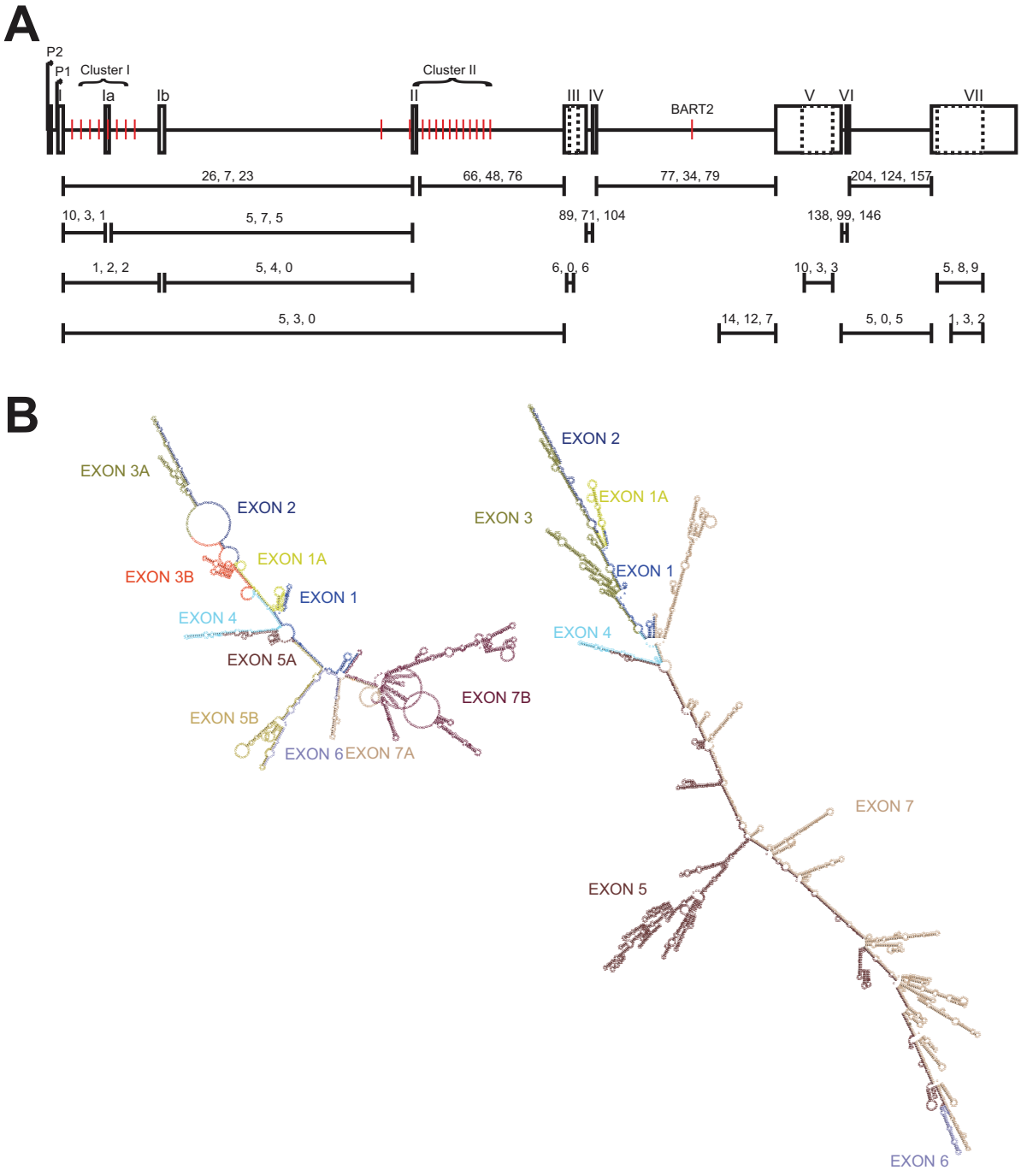

FIG 6 Splicing pattern of the BARTs obtained from RNA-seq. (A) Diagram of the BARTs drawn to scale, with boxes indicating exons and a connecting line indicating introns. The positions of the BART miRNAs are indicated by red vertical lines. Dotted lines within the exon boxes indicate alternative splicing events. Indicated below are the number of reads that span exon-exon junctions in each of the three libraries of AGS-EBV cells. These data suggest that the most common splicing pattern for the BARTs includes exons 1, 2, 3, 4, 5, 6, and 7 without the alternative splicing events that occur within exons 3, 5, and 7. It also suggests that there is much greater variation in the splicing pattern near the N terminus of the transcripts. Only splicing events that occurred at least five times across the three libraries are illustrated. (B) The RNAfold Webserver was used to generate minimum free energy predicted structures for the RNA encoded by the BART cDNA cloned in this study (left) and a BART RNA without alternative splicing in exons 3, 5, and 7 (right). Nucleotides are color coded by exon as indicated in order to better visualize from which part of the RNA the particular secondary structures are derived.

likely due to multiple changes in the transcriptional profile that occur during selection of stable lines, as well as the fact the pCEP4 vectors also express EBNA1, which likely also mediates some effects on cellular transcription. However, the use of multiple cell lines for each type of vector allows us to isolate the consistent changes are solely dependent upon BART expression.

Analysis of both the integrating and the episomal cell lines revealed that the BART cDNA was responsible for a considerable

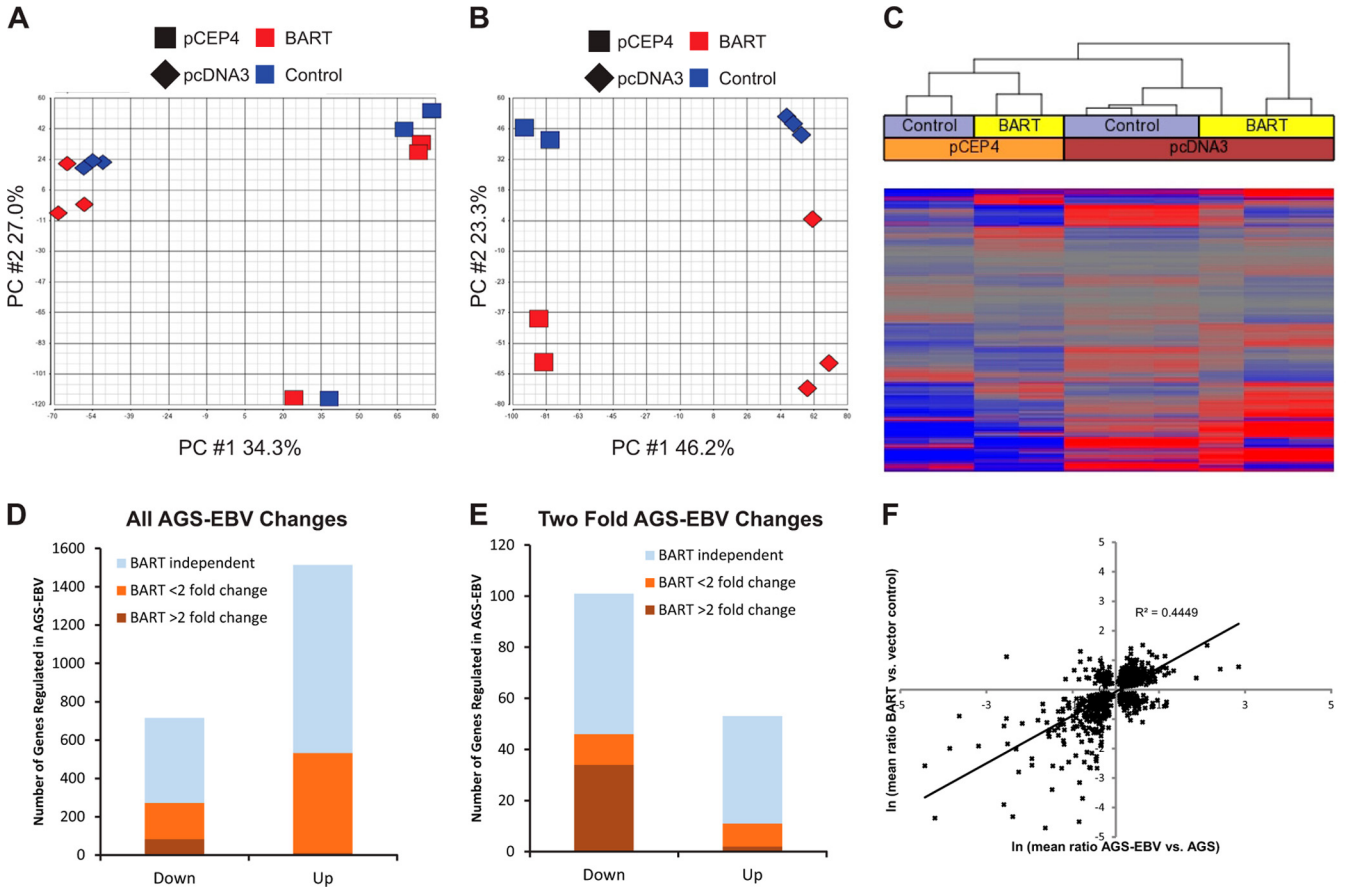

FIG 7 RNA-seq analysis of BART expressing cell lines. (A) Principle component analysis of variation between expressed transcripts from the six BART containing cell line transcription profiles, as well as the six vector control cell lines. Diamonds indicate pcDNA3 integrated stable cell lines, and squares indicate pCEP4 episomal vector lines. BART expressing libraries are shown in red, and the vector controls are shown in blue. The squares at the bottom of the graph are the first set of pCEP4 lines (pCEP4#1 and pCEP4-BART#1) and were excluded from further analysis as outliers. (B) Principle component analysis was repeated, excluding the two outliers indicated in panel A. Principle component 1 (*x* axis) separates the samples based on integrating versus episomal vector, and principle component 2 (*y* axis) separates the samples based on BART expression. (C) Hierarchical clustering of genes significantly changed by BART expression. The 4,404 genes significantly changed ($P < 0.05$) following BART expression were clustered independently. Red indicates expression higher than the mean of the 10 libraries, and blue indicates expression lower than the mean. Clustering of the samples first separates the pcDNA3 samples from the pCEP4 samples and then the BART expression from the vector controls. (D) Overlap between the AGS-EBV changed genes and the BART changed genes. For the genes upregulated and downregulated in the AGS-EBV data set, the number of genes changed in the same direction >2-fold and <2-fold in the BART data set are indicated. (E) Analysis similar to that depicted in panel D, but only considering genes that changed >2-fold in the AGS-EBV cells. (F) Correlation between the AGS-EBV and BART data sets. For each gene that was significantly changed in both data sets, the mean ratio is plotted for the AGS-EBV cells on the *x* axis and the BART cells on the *y* axis. A linear trendline is shown that indicates the positive correlation between these two data sets with the associated R^2 value for the line.

number of consistent transcriptional changes (Fig. 7C). In total, there were 2,405 genes upregulated and 1,999 genes downregulated with a *P* value of <0.05 (see Table S3 in the supplemental material). Of those, 96 genes were upregulated, and 240 genes were downregulated >2-fold. Importantly, many of the genes regulated by the BART were also identified as genes regulated following EBV infection (Fig. 7D and E). Perhaps most striking is the fact that nearly 50% of the genes downregulated 2-fold after latent EBV infection were also downregulated in the BART data set with the majority of the changes at least 2-fold (Fig. 7E). In addition, by plotting the changes in expression in the AGS-EBV cells against the changes in expression due to BART expression, a strong positive correlation can be observed (Fig. 7F). Taken together, these data suggest that a subset of the changes in gene expression induced by latent EBV infection in AGS cells is due to the expression of the BART nuclear RNAs and suggests that the spliced BART transcripts function as lncRNAs and from this point onward are referred to as the BART lncRNA.

Given the large overlap between the genes downregulated by EBV infection and BART lncRNA expression, the function of the BART lncRNA in downregulating specific cellular genes was confirmed by qRT-PCR in six AGS-EBV cell lines (three of which had been profiled by RNA-seq, and three of which were not), as well as three independent sets of pCEP4 and pCEP4-BART lines that were not part of the RNA-seq data. Primers were designed for eight genes of interest that were strongly downregulated in both the AGS-EBV, as well as the BART RNA-seq data sets, and that would possibly contribute to the altered growth properties and IPA predicted pathways. These genes include PGC, a secreted gastric protease shown to be a tumor suppressor in the context of gastric cancer. The proapoptotic gene RNF144B and the angiogenesis factor VEGFA were analyzed in addition to genes involved

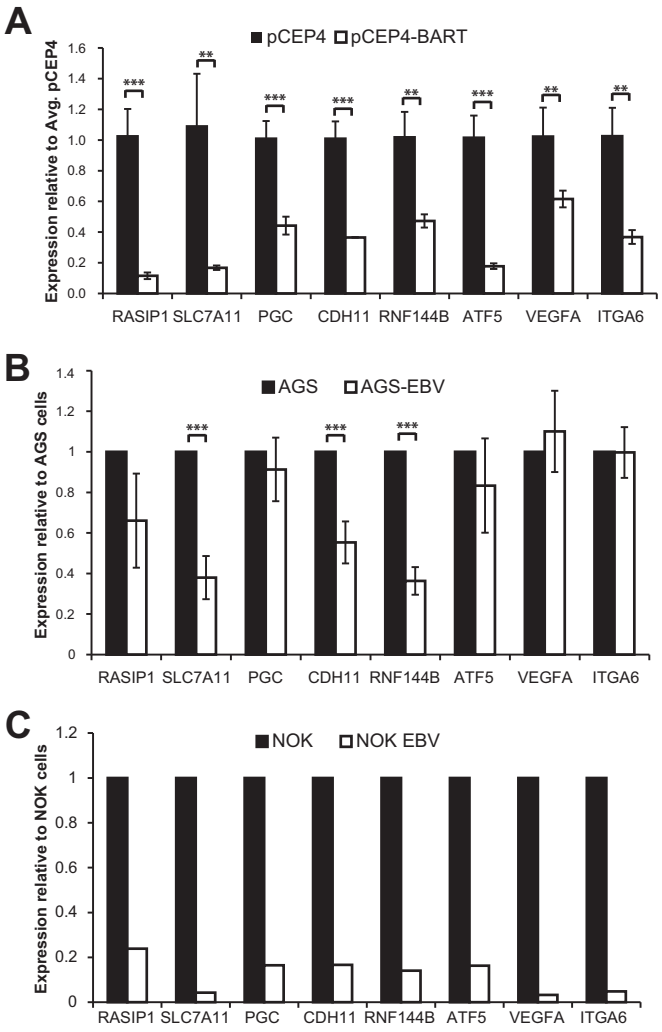

FIG 8 Confirmation of BART lncRNA downregulation of cellular genes by RT-PCR. (A) Quantitative RT-PCR was performed from RNA harvested from pCEP4 or pCEP4-BART AGS cell lines on the indicated genes. Assays were performed on three independent sets of cell lines, and expression was normalized first to a GAPDH control, and the mean result from pCEP4 for each gene was set to 1. The error bars represent the SEM. The asterisks refer to the results of a Student *t* test between the pCEP4 and pCEP4-BART samples (**, $P < 0.05$; ***, $P < 0.01$). (B) Quantitative RT-PCR was performed as for panel A from AGS cells and six independent AGS-EBV cell lines. Graphed is the mean result from two RNA preps from AGS cells, as well as each of the AGS-EBV cell lines with the error bars and a Student *t* test as in panel A. (C) Quantitative RT-PCR was performed as in panel A from NOK and NOK-EBV cells.

in the unfolded protein response (ATF5 and SLC7A11) and cell adhesion and migration (RASIP1, CDH11, VEGFA, and ITGA6). The expression of all eight of these genes was greatly decreased in the independently derived pCEP4-BART lines, suggesting that these results are highly reproducible (Fig. 8A). In addition, several of these genes were also significantly decreased across all of the AGS-EBV cell lines analyzed by RT-PCR, further suggesting a common mechanism of function for the BART lncRNAs in AGS cells (Fig. 8B). To determine whether these same genes were affected by EBV in another epithelial cell line, normal oral keratinocytes (NOKs) infected with EBV-Akata were analyzed. All eight of these genes were also downregulated in NOKs following EBV infection (Fig. 8C). Many of these genes, including RASIP1, SLC7A11, CDN11, and ITGA6, were also downregulated in the EBV-infected NPC cell line C666 that expresses high levels of the BARTs compared to an EBV-negative NPC cell line (29).

DISCUSSION

Despite the high prevalence of gastric cancer throughout the world and the clear association of latent EBV infection in a substantial subset of this tumor, relatively little research has addressed the mechanism through which the greatly restricted viral expression that is characteristic of this tumor promotes tumor formation. One of the biggest obstacles in studying EBV-positive gastric carcinomas is the lack of readily available EBV-positive gastric carcinoma cell lines and appropriate control cells for comparison. In the present study, infection of an EBV-negative gastric carcinoma cell line *in vitro* was used to address the specific contributions of latent viral infection to transformation. This model has the advantage of adopting the same restricted type I latency pattern as EBV-positive tumors, which is characterized by very limited protein expression (4). Analysis of the transcriptional changes induced by EBV infection of AGS cells predicted increased cellular proliferation and decreased apoptosis, which are consistent with anchorage-independent transformation. We provide here evidence that at least two classes of noncoding RNAs, the BART miRNAs and the spliced and polyadenylated BART nuclear RNAs derived from the same primary transcripts from the BamHI A region of the viral genome, both contribute to the reprogramming of the host cell gene expression. Importantly, the data presented are the first evidence that the BART spliced RNAs are functional, despite not being translated, presumably through mechanisms analogous to human lncRNAs.

An additional important finding of this sequencing study was identification of myc activation during EBV latency in AGS cells. This was first predicted by an analysis of the transcriptional changes and then confirmed using a myc-responsive luciferase promoter. EBV type I latency is characteristic of Burkitt lymphoma, where myc is activated through translocation (30). In type III latency, EBNA2 is known to directly activate c-myc through transcriptional activation (31). In contrast, in AGS cell latency, EBNA2 protein is not expressed (4), and transcriptional activation of c-myc was not detected by RNA-seq. Considering that the expression of the BART miRNAs is considerably higher in gastric cancer than in BL and thus presumably so is the BART lncRNA (32), this potentially indirect mechanism of activation may be specifically relevant in epithelial cells which have high levels of the BARTs. Interestingly, one of the downregulated genes that responded in the 3′UTR assay was the negative regulator of myc, MXI1. Thus, effects on MXI1 may be at least partially responsible for this increase in myc activity. In addition, EBV infection in AGS cells has been shown to decrease expression of the let-7 family of miRNAs (15) which directly regulate myc translation (33, 34). However, the myc protein levels were not consistently affected in the AGS-EBV cell lines, suggesting that the effect of decreased let-7 miRNA is unlikely to be the sole explanation for the increase in myc activity. It is likely that multiple factors contribute to this important phenotype of myc activation.

Expression of the BARTs represents the vast majority of polyadenylated viral transcription in gastric cancer (13, 14), and a correlated high expression of the BART miRNAs was also observed in these tumors (32, 35). Multiple studies have begun to

define the role of the BART miRNAs in the transformation ability of the virus. A naturally occurring deletion variant of EBV, B95-8, lacks most of the BART region (36) and a recombinant EBV lacking all viral miRNAs are still able to transform primary B lymphocytes *in vitro*, suggesting the BART miRNAs are not required for transformation of B cells (37). However, a recent study has suggested that expression of the BART miRNAs alone in AGS cells can promote tumor growth when the cells are passaged in mice, suggesting these miRNAs have transforming properties in epithelial cells *in vivo* (38). Evidence in the present study suggests that the ability of latent EBV infection to alter the growth of AGS cells also likely reflects expression of the BART miRNAs as the downregulated transcripts observed by RNA-seq are enriched in predicted BART miRNA targets. Several of these genes are important tumor suppressors, and the data presented here reveals that eight such genes are regulated at the level of the 3′UTR by EBV infection, strongly implying a role for the BART miRNAs. However, RNA-seq analysis revealed that the BART lncRNA also had a significant effect in the transcriptional reprogramming associated with latent EBV infection in these cells. Cloning and expression of the first full-length cDNA clone of a BART induced expression changes that largely mimicked a subset of the changes that occurred during EBV latent infection. This is particularly impressive considering that the cDNA expressed represents only one of multiple splice isoforms present during latent infection. Future studies will potentially delineate distinct functions for the other splice isoforms of the BART lncRNAs. Interestingly, the one tumor suppressor that did not respond in the 3′UTR assay, RASA1, was downregulated in response to BART lncRNA expression, suggesting that it is the lncRNA and not the miRNAs that is responsible for regulation of this gene. RASA1 is likely to be particularly important as it is a negative regulator of the ras oncogene. Interestingly, RASA1 mutations have been shown to be prevalent in EBV-negative gastric cancers (14).

The RNA-seq analysis presented here suggests that EBV infection and the BART lncRNAs regulate genes involved in the unfolded protein response (UPR). IPA of the AGS-EBV RNA-seq data suggested that XBP1 may be downregulated since many of the targets of XBP1 are decreased following EBV infection. XBP1 is one of three master regulatory transcription factors that make up the UPR, along with ATF4 and ATF6 (24). Additionally, XBP1 also functions in adaptive immunity since it is required for plasma cell differentiation (39). EBV reactivation that occurs upon plasma cell differentiation is regulated by XBP1, which can activate the promoter of the immediate-early gene, BZLF1 (40). This leads to the interesting hypothesis that in EBV epithelial latency the virus is suppressing XBP1 activity in order to remain latent. However, the level of XBP1 was unchanged in the RNA-seq data set and analysis of the splicing pattern indicated that the expressed XBP1 is the unspliced and thus less active splice variant. In addition, induction of ER stress in the AGS cells resulted in activation of XBP1 and the switch to the spliced variant, which occurred equally in both uninfected and infected cells. Thus, the predicted inhibition of the UPR was not due to effects on XBP1. However, in both the AGS-EBV and BART expressing AGS cells, both ATF5 and ATF6 had decreased expression. ATF6 is one of the three key transcription factors known to activate transcription in response to ER stress and ATF5 is another stress response transcription factor that responds to amino acid limitation through a mechanism analogous to ATF4 (41). Potential direct or indirect effects on these key regulators of the UPR by the BART lncRNAs are likely responsible for the subsequent decrease observed in stress responsive genes in the AGS-EBV cells.

Human lncRNAs have been shown to have a diverse array of functions. Nuclear lncRNAs often regulate transcription through directing epigenetic modifications to distinct regions of the chromatin (18). Additional studies will be required to understand the mechanism by which the BART lncRNAs modulate expression to downregulate a distinct subset of genes during EBV epithelial latency. Perhaps the mostly widely recognized strategy used by lncRNAs for the silencing of genes is disposition of the H3K27me3 mark through the recruitment of the polycomb repressive complex 2 (PRC2) (42). Alternatively, one prominent feature well established for EBV-positive gastric carcinomas is an extremely high level of CpG island promoter methylation that also results in the silencing of many important genes (14, 43, 44). It is tempting to speculate that the BART lncRNAs may affect histone regulation or potentially contribute to directing the DNA methylation phenotype. Many other mechanisms of transcriptional regulation are possible, and several have been ascribed to lncRNAs. The continued study of the function of these viral transcripts will likely yield new insights into the role of EBV in promoting growth and transformation of epithelial cells and also to the potential functions of lncRNAs.

ACKNOWLEDGMENTS

We thank Lindsey Hutt-Fletcher for supplying the infected AGS cell line and Shannon Kenney for providing the infected NOK cell line. We also thank the UNC Lineberger Genomics Core and the UNC High Throughput Sequencing Facility for library preparation and sequencing, respectively.

This study was supported by grants CA138811, CA 32979, and CA19014 from the National Institutes of Health to N.R.-T.

REFERENCES

1. **Longnecker RM, Cohen JI.** 2013. Epstein-Barr virus, p 1898–1959. *In* Knipe DM, Howley PM (ed), Fields virology, 6th ed. Lippincott/Williams & Wilkins, Philadelphia, PA.
2. **Raab-Traub N.** 2002. Epstein-Barr virus in the pathogenesis of NPC. Semin Cancer Biol **12:**431–441. http://dx.doi.org/10.1016/S1044579X0200086X.
3. **Raab-Traub N, Flynn K.** 1986. The structure of the termini of the Epstein-Barr virus as a marker of clonal cellular proliferation. Cell **47:**883–889. http://dx.doi.org/10.1016/0092-8674(86)90803-2.
4. **Marquitz AR, Mathur A, Shair KH, Raab-Traub N.** 2012. Infection of Epstein-Barr virus in a gastric carcinoma cell line induces anchorage independence and global changes in gene expression. Proc Natl Acad Sci U S A **109:**9593–9598. http://dx.doi.org/10.1073/pnas.1202910109.
5. **Raab-Traub N, Hood R, Yang CS, Henry B, II, Pagano JS.** 1983. Epstein-Barr virus transcription in nasopharyngeal carcinoma. J Virol **48:**580–590.
6. **Sadler RH, Raab-Traub N.** 1995. Structural analyses of the Epstein-Barr virus BamHI A transcripts. J Virol **69:**1132–1141.
7. **Thornburg NJ, Kusano S, Raab-Traub N.** 2004. Identification of Epstein-Barr virus RK-BARF0-interacting proteins and characterization of expression pattern. J Virol **78:**12848–12856. http://dx.doi.org/10.1128/JVI.78.23.12848-12856.2004.
8. **Al-Mozaini M, Bodelon G, Karstegl CE, Jin B, Al-Ahdal M, Farrell PJ.** 2009. Epstein-Barr virus BART gene expression. J Gen Virol **90:**307–316. http://dx.doi.org/10.1099/vir.0.006551-0.
9. **Pfeffer S, Zavolan M, Grasser FA, Chien M, Russo JJ, Ju J, John B, Enright AJ, Marks D, Sander C, Tuschl T.** 2004. Identification of virus-encoded microRNAs. Science **304:**734–736. http://dx.doi.org/10.1126/science.1096781.
10. **Cai X, Schafer A, Lu S, Bilello JP, Desrosiers RC, Edwards R, Raab-Traub N, Cullen BR.** 2006. Epstein-Barr virus microRNAs are evolution-

arily conserved and differentially expressed. PLoS Pathog **2:**e23. http://dx.doi.org/10.1371/journal.ppat.0020023.
11. **Zhu JY, Pfuhl T, Motsch N, Barth S, Nicholls J, Grasser F, Meister G.** 2009. Identification of novel Epstein-Barr virus microRNA genes from nasopharyngeal carcinomas. J Virol **83:**3333–3341. http://dx.doi.org/10.1128/JVI.01689-08.
12. **Edwards RH, Marquitz AR, Raab-Traub N.** 2008. Epstein-Barr virus BART microRNAs are produced from a large intron prior to splicing. J Virol **82:**9094–9106. http://dx.doi.org/10.1128/JVI.00785-08.
13. **Strong MJ, Xu G, Coco J, Baribault C, Vinay DS, Lacey MR, Strong AL, Lehman TA, Seddon MB, Lin Z, Concha M, Baddoo M, Ferris M, Swan KF, Sullivan DE, Burow ME, Taylor CM, Flemington EK.** 2013. Differences in gastric carcinoma microenvironment stratify according to EBV infection intensity: implications for possible immune adjuvant therapy. PLoS Pathog **9:**e1003341. http://dx.doi.org/10.1371/journal.ppat.1003341.
14. **Cancer Genome Atlas Research Network.** 2014. Comprehensive molecular characterization of gastric adenocarcinoma. Nature **513:**202–209. http://dx.doi.org/10.1038/nature13480.
15. **Marquitz AR, Mathur A, Chugh PE, Dittmer DP, Raab-Traub N.** 2014. Expression profile of microRNAs in Epstein-Barr virus-infected AGS gastric carcinoma cells. J Virol **88:**1389–1393. http://dx.doi.org/10.1128/JVI.02662-13.
16. **Kassis J, Maeda A, Teramoto N, Takada K, Wu C, Klein G, Wells A.** 2002. EBV-expressing AGS gastric carcinoma cell sublines present increased motility and invasiveness. Int J Cancer **99:**644–651. http://dx.doi.org/10.1002/ijc.10382.
17. **Mercer TR, Mattick JS.** 2013. Structure and function of long noncoding RNAs in epigenetic regulation. Nat Structural Mol Biol **20:**300–307. http://dx.doi.org/10.1038/nsmb.2480.
18. **Batista PJ, Chang HY.** 2013. Long noncoding RNAs: cellular address codes in development and disease. Cell **152:**1298–1307. http://dx.doi.org/10.1016/j.cell.2013.02.012.
19. **Wille CK, Nawandar DM, Panfil AR, Ko MM, Hagemeier SR, Kenney SC.** 2013. Viral genome methylation differentially affects the ability of BZLF1 versus BRLF1 to activate Epstein-Barr virus lytic gene expression and viral replication. J Virol **87:**935–950. http://dx.doi.org/10.1128/JVI.01790-12.
20. **Hermeking H, Rago C, Schuhmacher M, Li Q, Barrett JF, Obaya AJ, O'Connell BC, Mateyak MK, Tam W, Kohlhuber F, Dang CV, Sedivy JM, Eick D, Vogelstein B, Kinzler KW.** 2000. Identification of CDK4 as a target of c-MYC. Proc Natl Acad Sci U S A **97:**2229–2234. http://dx.doi.org/10.1073/pnas.050586197.
21. **Robinson JT, Thorvaldsdottir H, Winckler W, Guttman M, Lander ES, Getz G, Mesirov JP.** 2011. Integrative genomics viewer. Nat Biotechnol **29:**24–26. http://dx.doi.org/10.1038/nbt.1754.
22. **Mainou BA, Everly DN, Jr, Raab-Traub N.** 2005. Epstein-Barr virus latent membrane protein 1 CTAR1 mediates rodent and human fibroblast transformation through activation of PI3K. Oncogene **24:**6917–6924. http://dx.doi.org/10.1038/sj.onc.1208846.
23. **Concha M, Wang X, Cao S, Baddoo M, Fewell C, Lin Z, Hulme W, Hedges D, McBride J, Flemington EK.** 2012. Identification of new viral genes and transcript isoforms during Epstein-Barr virus reactivation using RNA-Seq. J Virol **86:**1458–1467. http://dx.doi.org/10.1128/JVI.06537-11.
24. **Hetz C, Chevet E, Harding HP.** 2013. Targeting the unfolded protein response in disease. Nat Rev Drug Discov **12:**703–719. http://dx.doi.org/10.1038/nrd3976.
25. **Gottwein E, Corcoran DL, Mukherjee N, Skalsky RL, Hafner M, Nusbaum JD, Shamulailatpam P, Love CL, Dave SS, Tuschl T, Ohler U, Cullen BR.** 2011. Viral microRNA targetome of KSHV-infected primary effusion lymphoma cell lines. Cell Host Microbe **10:**515–526. http://dx.doi.org/10.1016/j.chom.2011.09.012.
26. **Kang D, Skalsky RL, Cullen BR.** 2015. EBV BART MicroRNAs target multiple proapoptotic cellular genes to promote epithelial cell survival. PLoS Pathog **11:**e1004979. http://dx.doi.org/10.1371/journal.ppat.1004979.
27. **Marquitz AR, Raab-Traub N.** 2012. The role of miRNAs and EBV BARTs in NPC. Semin Cancer Biol **22:**166–172. http://dx.doi.org/10.1016/j.semcancer.2011.12.001.
28. **Cao S, Strong MJ, Wang X, Moss WN, Concha M, Lin Z, O'Grady T, Baddoo M, Fewell C, Renne R, Flemington EK.** 2015. High-throughput RNA sequencing-based virome analysis of 50 lymphoma cell lines from the Cancer Cell Line Encyclopedia project. J Virol **89:**713–729. http://dx.doi.org/10.1128/JVI.02570-14.
29. **Szeto CY, Lin CH, Choi SC, Yip TT, Ngan RK, Tsao GS, Li Lung M.** 2014. Integrated mRNA and microRNA transcriptome sequencing characterizes sequence variants and mRNA-microRNA regulatory network in nasopharyngeal carcinoma model systems. FEBS Open Bio **4:**128–140. http://dx.doi.org/10.1016/j.fob.2014.01.004.
30. **Rowe M, Kelly GL, Bell AI, Rickinson AB.** 2009. Burkitt's lymphoma: the Rosetta Stone deciphering Epstein-Barr virus biology. Semin Cancer Biol **19:**377–388. http://dx.doi.org/10.1016/j.semcancer.2009.07.004.
31. **Kaiser C, Laux G, Eick D, Jochner N, Bornkamm GW, Kempkes B.** 1999. The proto-oncogene c-myc is a direct target gene of Epstein-Barr virus nuclear antigen 2. J Virol **73:**4481–4484.
32. **Qiu J, Cosmopoulos K, Pegtel M, Hopmans E, Murray P, Middeldorp J, Shapiro M, Thorley-Lawson DA.** 2011. A novel persistence associated EBV miRNA expression profile is disrupted in neoplasia. PLoS Pathog **7:**e1002193. http://dx.doi.org/10.1371/journal.ppat.1002193.
33. **Akao Y, Nakagawa Y, Naoe T.** 2006. let-7 microRNA functions as a potential growth suppressor in human colon cancer cells. Biol Pharm Bull **29:**903–906. http://dx.doi.org/10.1248/bpb.29.903.
34. **Sampson VB, Rong NH, Han J, Yang Q, Aris V, Soteropoulos P, Petrelli NJ, Dunn SP, Krueger LJ.** 2007. MicroRNA let-7a downregulates MYC and reverts MYC-induced growth in Burkitt lymphoma cells. Cancer Res **67:**9762–9770. http://dx.doi.org/10.1158/0008-5472.CAN-07-2462.
35. **Kim do, N, Chae HS, Oh ST, Kang JH, Park CH, Park WS, Takada K, Lee JM, Lee WK, Lee SK.** 2007. Expression of viral microRNAs in Epstein-Barr virus-associated gastric carcinoma. J Virol **81:**1033–1036. http://dx.doi.org/10.1128/JVI.02271-06.
36. **Raab-Traub N, Dambaugh T, Kieff E.** 1980. DNA of Epstein-Barr virus VIII: B95-8, the previous prototype, is an unusual deletion derivative. Cell **22:**257–267. http://dx.doi.org/10.1016/0092-8674(80)90173-7.
37. **Seto E, Moosmann A, Gromminger S, Walz N, Grundhoff A, Hammerschmidt W.** 2010. Micro RNAs of Epstein-Barr virus promote cell cycle progression and prevent apoptosis of primary human B cells. PLoS Pathog **6:**e1001063. http://dx.doi.org/10.1371/journal.ppat.1001063.
38. **Qiu J, Smith P, Leahy L, Thorley-Lawson DA.** 2015. The Epstein-Barr virus encoded BART miRNAs potentiate tumor growth in vivo. PLoS Pathog **11:**e1004561. http://dx.doi.org/10.1371/journal.ppat.1004561.
39. **Reimold AM, Iwakoshi NN, Manis J, Vallabhajosyula P, Szomolanyi-Tsuda E, Gravallese EM, Friend D, Grusby MJ, Alt F, Glimcher LH.** 2001. Plasma cell differentiation requires the transcription factor XBP-1. Nature **412:**300–307. http://dx.doi.org/10.1038/35085509.
40. **Bhende PM, Dickerson SJ, Sun X, Feng WH, Kenney SC.** 2007. X-box-binding protein 1 activates lytic Epstein-Barr virus gene expression in combination with protein kinase D. J Virol **81:**7363–7370. http://dx.doi.org/10.1128/JVI.00154-07.
41. **Zhou D, Palam LR, Jiang L, Narasimhan J, Staschke KA, Wek RC.** 2008. Phosphorylation of eIF2 directs ATF5 translational control in response to diverse stress conditions. J Biol Chem **283:**7064–7073. http://dx.doi.org/10.1074/jbc.M708530200.
42. **Margueron R, Reinberg D.** 2011. The Polycomb complex PRC2 and its mark in life. Nature **469:**343–349. http://dx.doi.org/10.1038/nature09784.
43. **Kang GH, Lee S, Kim WH, Lee HW, Kim JC, Rhyu MG, Ro JY.** 2002. Epstein-barr virus-positive gastric carcinoma demonstrates frequent aberrant methylation of multiple genes and constitutes CpG island methylator phenotype-positive gastric carcinoma. Am J Pathol **160:**787–794. http://dx.doi.org/10.1016/S0002-9440(10)64901-2.
44. **Vo QN, Geradts J, Gulley ML, Boudreau DA, Bravo JC, Schneider BG.** 2002. Epstein-Barr virus in gastric adenocarcinomas: association with ethnicity and CDKN2A promoter methylation. J Clin Pathol **55:**669–675. http://dx.doi.org/10.1136/jcp.55.9.669.